國 立 交 通 大 學

機械工程學系

碩士論文

以電鍍鎳-鑽石奈米複材改進梳狀致動器性能之研究

Performance Enhancement of Comb Drive Actuators Utilizing

Electroplating of Nickel-Diamond Nanocomposite

研 究 生：李毅家

指導教授：鄭裕庭　博士

徐文祥　博士

中華名國九十四年六月

以電鍍鎳-鑽石奈米複材改進梳狀致動器性能之研究

Performance Enhancement of Comb Drive Actuators Utilizing

Electroplating of Nickel-Diamond Nanocomposite

研 究 生：李毅家　　　　　　　Student：Yi-Chia Lee

指導教授：鄭裕庭　　　　　　　Advisor：Yu-Ting Cheng

　　　　　徐文祥　　　　　　　　　　　　Wensyang Hsu

國立交通大學

機械工程學系

碩士論文

A Thesis
Submitted to Department of Mechanical Engineering
College of Engineering
National Chiao Tung University
In Partial Fulfillment of the Requirements
For the Degree of Master
in
Mechanical Engineering
June 2005
Hsinchu, Taiwan, Republic of China

中華民國九十四年六月

以電鍍鎳–鑽石奈米複材改進梳狀致動器性能之研究

學生：李毅家　　　　　　　　　　　　　指導教授：鄭裕庭

　　　　　　　　　　　　　　　　　　　　　　徐文祥

國立交通大學機械工程學系　碩士班

摘　　　要

　　在微機電的研究領域之中，常以矽作為元件之材料。由材料的觀點出發，矽本身擁有優良的機械性質；但導電之性質必須藉由摻雜來提升。在製程方面，矽之操作溫度偏高，導致以其所製作之元件與電路難以整合。反觀金屬本身即具有導電特性；製程上，可藉由電鍍獲得所需結構，操作溫度接近室溫，此項特性大大提升元件與電路之間的整合性。

　　由相關的研究發現，在金屬鎳中添加奈米粉末，可以改變鎳之部分機械性質，例如在鎳中加入奈米等級的鑽石粒子，可以增加鎳之楊氏係數，根據此結果，將其應用於梳狀致動器上，使其比純鎳所製作之梳狀致動器擁有更高的共振頻率。

　　在製程方面，以往電鍍之梳狀致動器容易產生挫曲的結構。在此，調整電鍍參數以改變結構之內應力，其中包括電流密度與操作溫度兩大重要參數，將其調整至 $1.2mA/cm^2$，35 即可解決內應力造成之結構挫曲問題。

　　在量測結果方面，以奈米壓痕器量測純鎳以及鎳–鑽石鍍膜，發現楊氏係數由 173GPa 提升至 217GPa。在共振頻率量測方面，針對純鎳與在電鍍液中添加 2g/L 的鑽石奈米粉末兩種不同材料所製作之梳狀致動器。發現第一模態的頻率由 8.034kHz 移至 8.949kHz，提升了 11.3%，與模擬所得之 10.2%提升量之數值接近，驗證了鑽石奈米粉末可提升電鍍鎳之梳狀致動器之共振頻率。

Performance Enhancement of Comb Drive Utilizing Electroplating of Nickel-Diamond Nanocomposite

Student：Yi-Chia Lee   Advisors：Yu-Ting Cheng

Wensyang Hsu

Department of Mechanical Engineering

National Chiao Tung University

Abstract

In MEMS field, most devices are fabricated by silicon. Silicon provides good mechanical properties. The conductivity of silicon must be improved by doping process. The high temperature process of silicon makes MEMS devices difficult to integrate with IC. Comparing with silicon, metal doesn't need doping process. By electroplating, the problem of high temperature is solved because electroplating is a low temperature process.

In the previous researches, it is found that some kinds of nano particles change some mechanical properties of nickel. For example, diamond nano particles improve the Young's modulus of nickel. According to this characteristic, the comb drive made by nickel-diamond nanocomposite gets higher resonant frequency than pure nickel one.

The bending of comb drive is the biggest problem of fabrication process. It can be solved by tuning the parameters of electroplating conditions which include current density and operation temperature. Under 1.2mA/cm^2 and 35 , it is possible to get the structure with no bending.

The Young's modulus is measured by nano indenter. For diamond concentration of 2g/L, the diamond nano particles improve the Young's modulus of nickel from 173GPa to

217GPa.　　The resonant frequency is measured by Laser Doppler Vibrometer.　　The frequency of first mode shifts from 8.034kHz to 8.949kHz.　　There is an 11.4% improvement. This value is close to 10.2% which is gotten by simulation.　　It is precisely on such grounds that diamond nanoparticles can improve the resonant frequency of comb drive made by electroplating nickel.

Acknowledgements

Contents

Figure Captions

Table Captions

Chapter 1 Introduction

1.1 Motivation

Over the past few years a considerable number of studies have been made on MEMS devices. On the basis of what are needed for MEMS devices, many kinds of fabrication processes which are developed from IC processes have been proposed. MUMPs is a notable example.

Most of these processes utilize silicon as the structure material. With the exception of silicon, metal is interested because of many superior material properties of it in certain applications. First, metal needn't doping process to improve the conductivity. Secondly, metal process is easier to achieve thick structure. Thirdly, it is easy to obtain metal structure at low temperature. High temperature process always brings the thermal stress issue. Thermal stress causes bending especially for suspended structures.

Nickel is one of the commonest metals applied to MEMS devices and it can be realized by electroplating. There are several articles which have been devoted to this study. Some of them point out that nickel with nanoparticles in it can improve specific properties. For example, nickel with diamond nanoparticles in it has higher Yung's modulus than pure nickel. It is helpful for nickel applied to RF devices because the higher Young's modulus improves the higher resonant frequency.

In MEMS application, comb drive is one of the most popular and famous microdevice. It is a good example of RF device which is designed and fabricated by MEMS fabrication processes.

Now using metal as the structural material, the performances of comb drive is decided by what is used as the structure material. Young's modulus and density are key properties

because they influence the resonant frequency deeply. Device fabricated with high E/ρ ratio material can obtain higher resonant frequency than others. So utilizing nickel-diamond nanocomposite as the structural material, comb drive will be fabricated by electroplating. Resonant frequency improvement of comb drive made by nickel will obtain by test.

1.2 Related Literature

1.2.1 Comb Drive with Silicon-Based

There were many literatures on comb drive. In 1989, comb-drive were reported by Tang et al [1]. The design of comb drive actuators is shown in Figure 1-1. The concept of actuation was using the relation between electrostatic force and spring force. Voltage was the input signal. Different voltage applied on the different combs and resulted in electrostatic force between active and immobile combs. After the balance between electrostatic force and spring force provided form the eight beams suspend on the two side of the active combs part, the output signal displacement was obtained. By matching the frequency of the input signal with the resonant frequency of comb drive structure, large displacement was obtained.

In order to improve the performance of comb drive actuators, many researches were published to show the ways to achieve it. Using comb drive as a resonator, the resonant frequency is the most important point needs to be improved. From the frequency equation, the frequency depends on the spring constant and the mass of the system. The spring constant and the mass of the system can be adjusted by the dimensions and the material of the structure. Actually, searching for the suitable materials is the main destination.

In Tang's fabrication process, low pressure chemical vapor deposition (LPCVD) polycrystalline silicon was utilized as the structural material [1]. The operation temperature

of LPCVD polycrystalline silicon was above 600 .   The high temperature process induced thermal stress and low deposition rate were the issues of polycrystalline silicon.   Biebl et al presented a method to improve the deposition rate, resistivity, and residual stress [2].   By controlling the ratio of phosphine to silane and rapid thermal annealing (RTA) process, the 42 Å/min deposition and 0.8mΩcm resistivity were obtained.   A cantilever beam with 2 μm in thickness and 1000μm in length showed an end deflection of less than 0.2μm.

Franke et al used polycrystalline germanium instead of polycrystalline silicon as structural material in 1999 [3].   The fabrication process included LPCVD and RTA. By this process, low resistivity and tensile polycrystalline germanium film was obtained.   The testing results showed that RTA process shifted the film stress form tensile to compressive. So by well control of deposition and annealing condition, the film stress could be minimized.

The polycrystalline silicides were bought up as the structural materials.   Tri-layer polycrystalline SiGe structure could reduce the strain gradient [4].   Polycrystalline SiC provided high Young's modulus up to 710 GPa [5].   These two materials both deposited by LPCVD and needed RTA process to reduce thermal stress.

Comb drives were made by surface micromachining in these literatures above.   There were some comb drives made by bulk micromachining.   The most popular example was using the SOI wafer to achieve it [6][7][8].   The thick silicon layer was utilized as the structure and fabricated by bulk micromachining, so the high aspect ratio combs were obtained.   This method was usually used as the vertical driving comb drive because it provided larger area for comb sidewall.
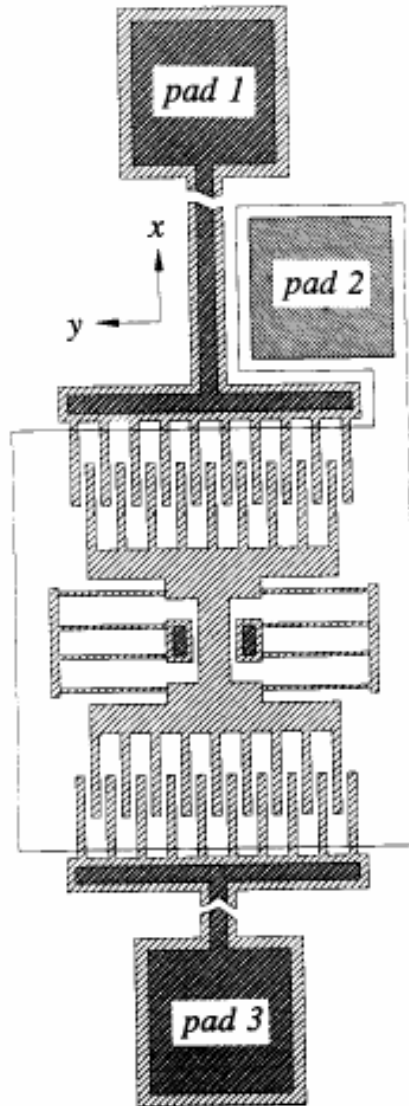
Figure 1-1 comb structures with spring beams on each side[1].

1.2.2 Nickel and Nickel Nanocomposite

Being a new technology, electroplating nickel provides many advantages. High deposition rate, easy stress control, low deposition temperature, and low resistivity are the advantages of electroplating nickel instead of polycrystalline silicon [9][10]. By choosing the suitable fabrication process, it is well suited for post processing on preprocessed CMOS wafers.

In the development of nano particles in metal, based on electroplating nickel, there were some materials being added into the solution of electroplating. In 2002, Teh et al used the ceramic particles as the additive to electroplate the nickel ceramic composite film [11]. Ceramic particles, either in the form of cordierite, or iron oxide, dispersed well within the solution. After fabrication of the nickel ceramic film, the testing result showed that composite film significantly reduced the mismatch of thermal expansion between nickel and silicon. Fortunately, the Young's modulus, Berkovich hardness, and electrical resistivity were maintained.

After nickel ceramic composite film, Teh et al used diamond and cordierite as the additive [12]. In Figure 1-2, the left microresonator was made by nickel and the right one was made by nickel cordierite. Obviously, the nickel cordierite microresonator was residual stress free because of the better thermal compatibility with silicon. By adding various concentration of diamond particles, it was found that higher diamond concentration obtained the film with more compressively stress.

In 2003, Tsai et al followed Teh's research and used nickel and diamond nanoparticles as the materials of electro-thermal microactuators [13]. The E/ρ ratio of microactuators could be enhanced 7.1 times with diamond concentration of 2 g/l. Comparing to device made of electroplated nickel, the microactuators with diamond concentration of 2 g/l could reduce 73% power requirement for 3μm displacement of cantilever beam.

The similar research is taken by Shen in 2004 [13]. The Ni-P-CNT and Ni-P-Diamond films are gotten by electroless. The E/ρ ratios reach 3.9 and 3 times for Ni-P-CNT and Ni-P-Diamond individually. The electrical conductivities are 1.903x10-6Ω-m and 1.399x10-6Ω-m.

Comparing metal-based with surface silicon-based micromachining, the deposition rate and thermal stress will be improved. Although using bulk silicon-based micromachining is good for the aspect ratio and the fabrication, it is not easy to integrate comb drive with IC

process and the cost SOI wafer is high. Using metal based process will solve these problems in bulk silicon-based micromachining.
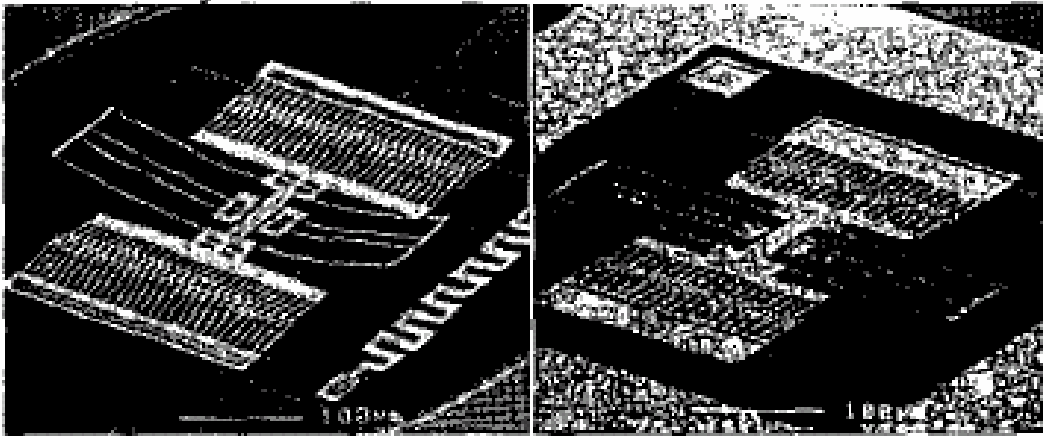
Figure 1-2 (a, left) a partially released nickel microresonator. (b, right) a full released nickel cordierite microresonator[12].

1.3 Current Approach

In previous researches, it is found that nickel-diamond nanocomposite can enhance the E/ρ ratio. As Figure 1-3 indicates, the E/ρ ratio can be enhanced 7.1 times with 2g/L diamond concentration. Basing on this enhancement, comb drive is used as the test device to demonstrate the application of nickel-diamond nanocomposite. The enhancement of the E/ρ ratio promotes the resonant frequency of comb drive.

The deposition method is electroplating. By adding diamond nano particles into the electroplating solution, the nickel-diamond nanocomposite can be deposited. In previous researches, it is sure that diamond nano particles are well dispersed within the nickel film.

In brief, the objective of this thesis is to demonstrate nickel-diamond nanocomposite can be used to fabricate comb drive and the resonant frequency is considered as the performance of comb drive to compare with pure nickel one.
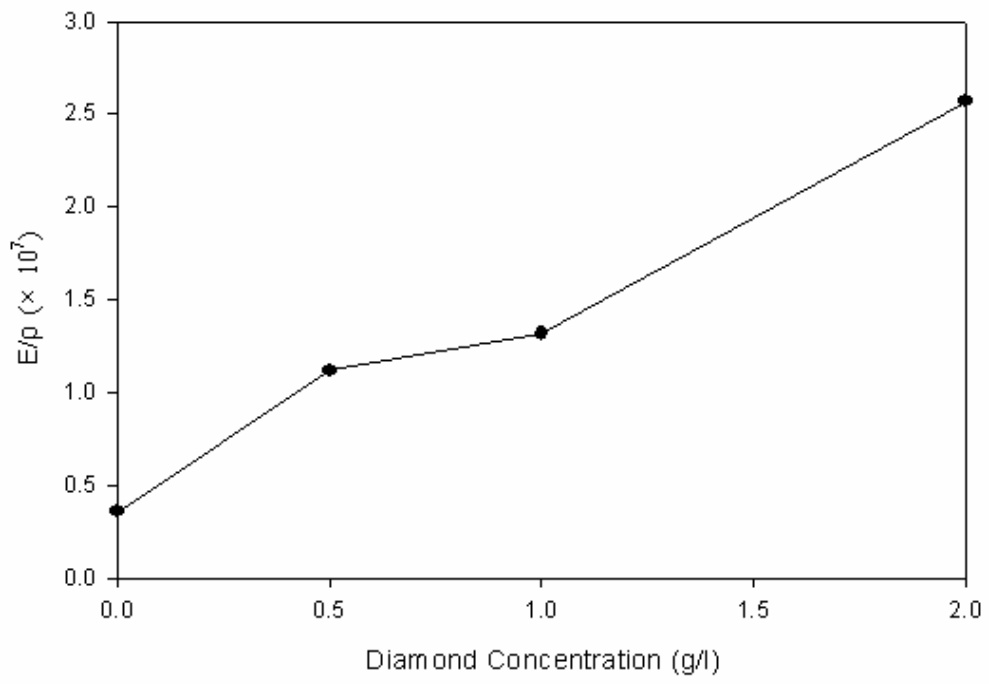
Figure 1-3 E/ρ-Diamond concentration [13].

Chapter 2 Design and Analysis

2.1 Design of Comb Drive

The structure of comb drive follows Tang's design. It is similar to what is shown in Figure 1-1 and the dimensions of comb drive are based on the fabrication ability. So the dimension is decided and the critical dimension of comb drive is shown in Table 2-1.

Table 2-1 the critical dimension of comb drive.

dimension	length (μm)	width (μm)	thickness (μm)
spring	300/250/200	10	7
comb	100	10	7

2.2 Analytic Solution and FEM Result

Comb drive can be considered as the spring-mass damping system and the resonant frequency can be written as the following equation:

$$f_r = \frac{1}{2\pi}\sqrt{\frac{K}{M}} \tag{2.1}$$

Where f_r is the resonant frequency of comb drive; K is the spring constant of comb drive; M is the effective mass of comb drive. The spring constant can be expressed as:

$$K = \frac{2EW^3t}{L^3} \tag{2.2}$$

Where W is the width of the spring. L and t are the length and the thickness individually. In the Tang's paper, the effective can be written into two parts, the suspension part and the spring.

8

$$M = M_p + 0.3714M_s \tag{2.3}$$

M_p and M_s are the mass of the suspension part and the spring.   According to (2.2) and (2.3), the equation can be rewritten as:

$$f_r = \frac{1}{2\pi}\sqrt{\frac{2EW^3 t}{L^3(M_p + 0.3714M_s)}} \tag{2.4}$$

In order to recognize the influence by the E/ρ ratio, the equation is written as:

$$f_r = \frac{1}{\sqrt{2}\pi}\sqrt{\frac{W^3}{L^3(A_p + 0.3714A_s)}}\sqrt{\frac{E}{\rho}} \tag{2.5}$$

A_p and A_s are the area of the suspension part and the spring.   It is easy to find out that the resonant frequency increases in direct proportion to the square root of the E/ρ ratio.

The resonant frequency of comb drive can be simulated by Ansys.   The model of comb drive by Ansys is shown in Figure 2-1.   There is one thing must be concerned.   The meshing size influences the result deeply.   The more accurate solution of resonant frequency can be obtained by using the smaller meshing size.   Only the critical parts need smaller meshing size.   So by Figure 2-1, the spring parts are meshed smaller than other part.

By equation (2.5) and FEM simulation, the resonant frequency of comb drive can be computed.   The result is shown in Table 2-2.
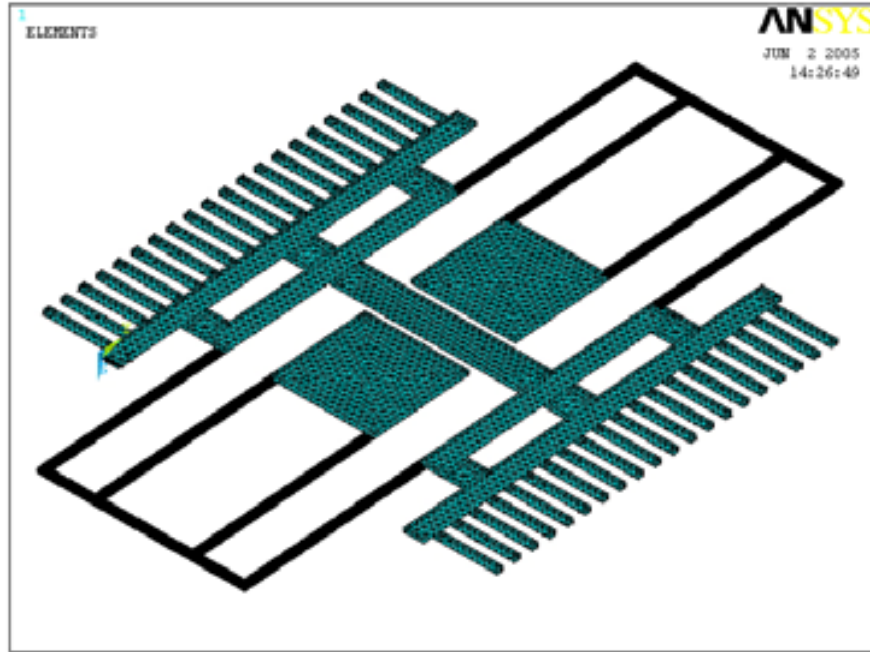
Figure 2-1 the model the comb drive by Ansys.

Table 2-2 analytical solution and FEM simulation of the resonant frequency.

Material Property			Length of spring (μm)	Resonant frequency(Hz)	
Material	E (GPa)	ρ (kg/m^3)		Analytical	simulation
Pure Nickel	190	8908	300	16829	15719
			250	22239	20347
			200	31246	27750
Nickel-Diamond	230	8882	300	18543	17319
			250	24504	22419
			200	34429	30576
Poly Silicon	169	2330	300	31033	28986
			250	41010	37521
			200	57621	51173

2.3 Modal Shape Discussion

By Ansys, the resonant frequency of comb drive is simulated. In the simulation results, it is found that the in-plane motion is the third mode. In other words, there are two modes with lower frequencies.

This phenomenon can be explained by the effective spring constant. In order to simplify the problem, the effective spring constant is considered as two parts: (in x direction) and K_z (in z direction). According to the dimension design of comb drive, K_z is less than K_x. The first mode and the second mode are torsional and out-of-plane. The effective spring constants of these two modes are contributed almost by K_z. The effective spring constants of torsional and out-of-plane motion are lower than in-plane motion. The lower effective spring constant gets lower resonant frequency. There are two modes with lower frequency before in-plane mode. The results are shown in Table 2-3.
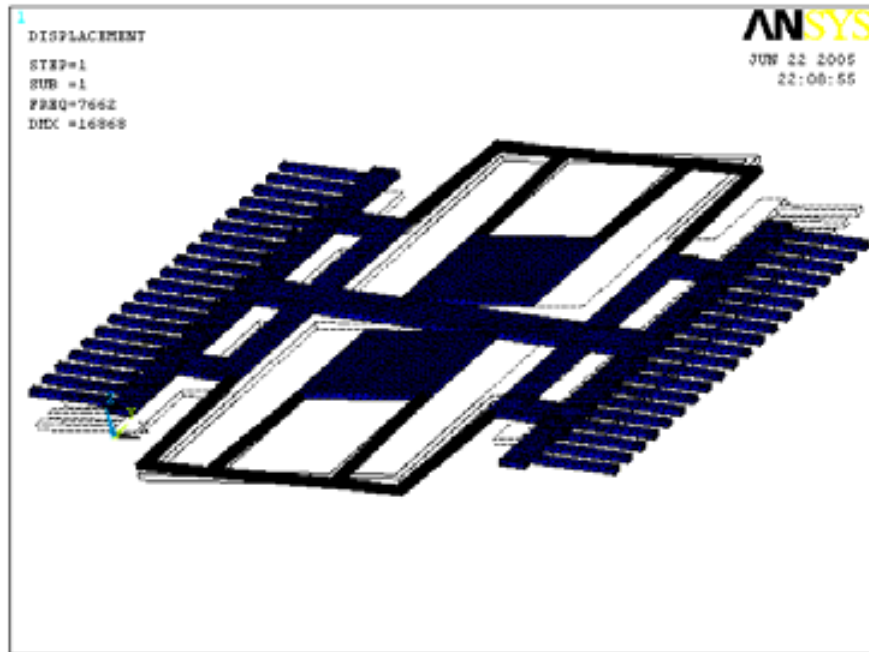
(a)
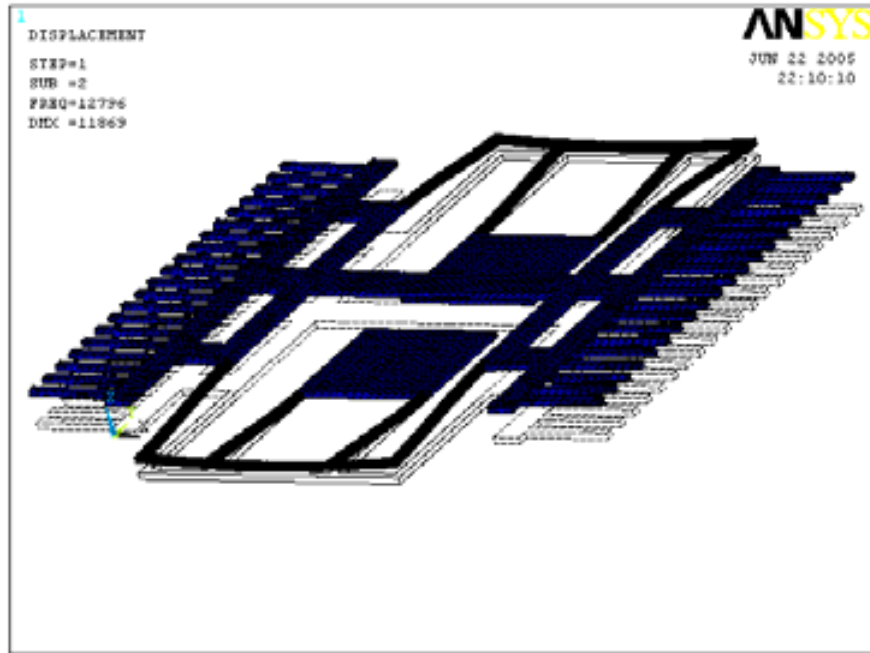
(b)
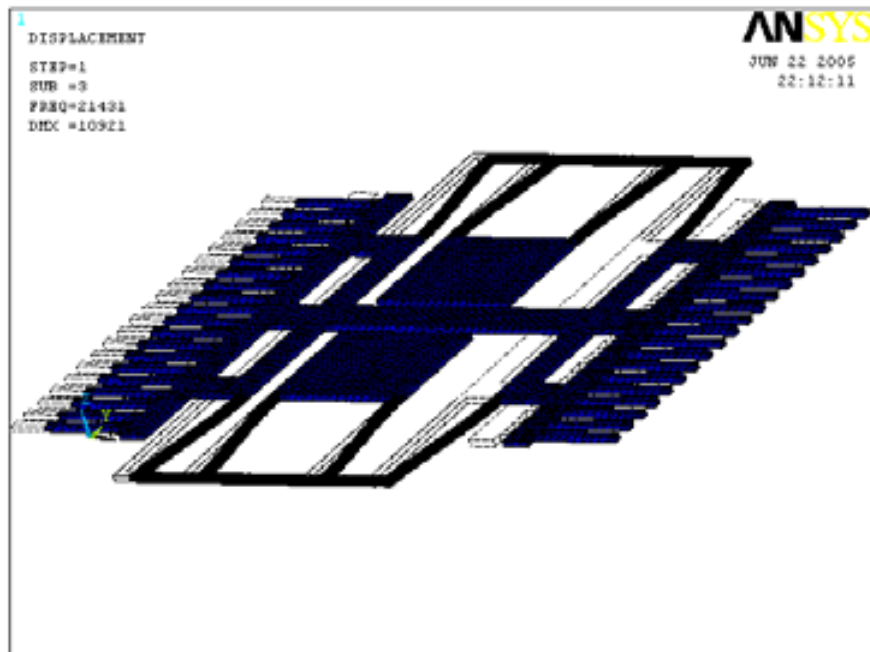
(c)

Figure 2-2 the (a) first mode; (b) second mode; (c) third mode of comb drive modal simulation.

Table 2-3 the resonance frequencies of pure nickel and nickel-diamond under different mode.

material	length of spring (μm)	mode (Hz)		
		1	2	3
pure nickel	300	6804	10261	15719
	250	8052	12847	20347
	200	9921	16569	27750
nickel-diamond	300	7497	11306	17319
	250	8872	14156	22419
	200	10932	18257	30576
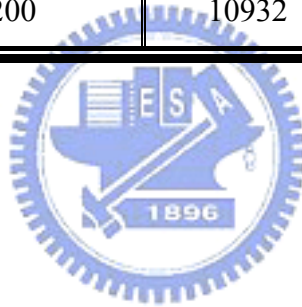
Chapter 3 Fabrication Process

3.1 Fabrication Process

The comb drive structure is shown in Figure 3-1.　There are three main layers: (1) pad, (2) sacrificial layer, (3) structure layer.　Here pad and structure layer are used nickel as the material.　Photoresist (PR) and copper are the choices for sacrificial layer.

Figure 3-1 the structure of the comb drive.

3.1.1 Sacrificial Layer

Before coming to the fabrication process, the sacrificial layer must be determined. Considering the thermal expansion coefficient variation with nickel and the fabrication method, there are two materials available, PR and copper.

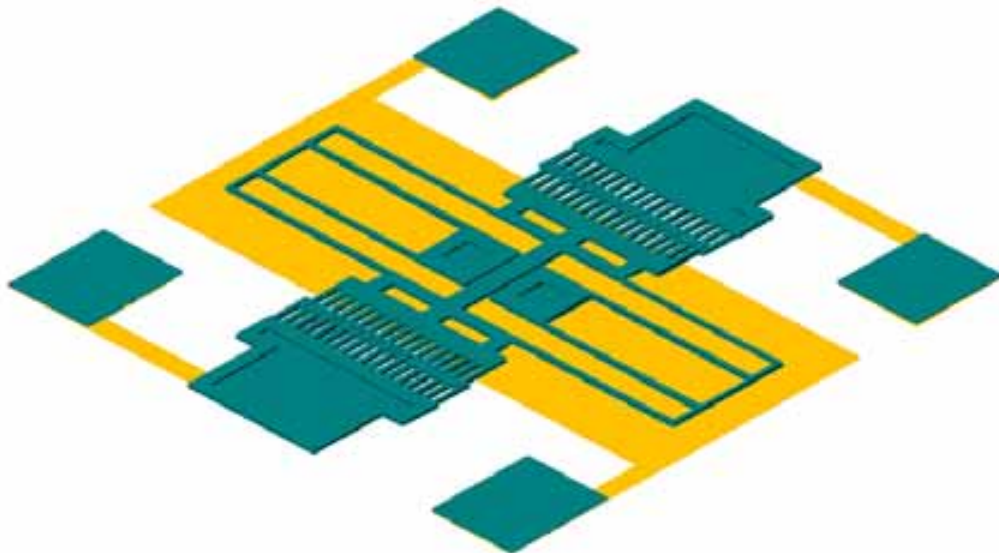Easy to handle is the advantage for PR.　It is easy to obtain any thickness by controlling

the rotation rate.   It also provides good uniformity.   The only thing that must be concerned

is the hard bake of PR.   Referring to Figure 3-1 and Figure 3-3, the PR sacrificial layers fail

because of no hard bake or hard bake less.   These damages occur at soft bake of next PR

process.   This problem can be solved by appropriate hard bake, but the hard bake causes the

sidewall reflow.   Fortunately, this phenomenon influences the post-process less.

There is no reflow with Cu sacrificial layer.   So it is easy to obtain vertical sidewall.

The Cu sacrificial layer is shown in Figure 3-4.   The uniformity is the biggest problem of

this process.   This Cu layer is deposited by electroplating.   Comparing to PR, it is harder

for electroplating Cu to obtain a uniform surface.   From the profile figure in Figure 3-5, it is

useful to obtain good uniformity by reducing the current density.

Comparing PR with Cu, PR process need less time than Cu process, but Cu sacrificial is

more suitable for post-process than PR.   To sum up, these two materials are both suitable
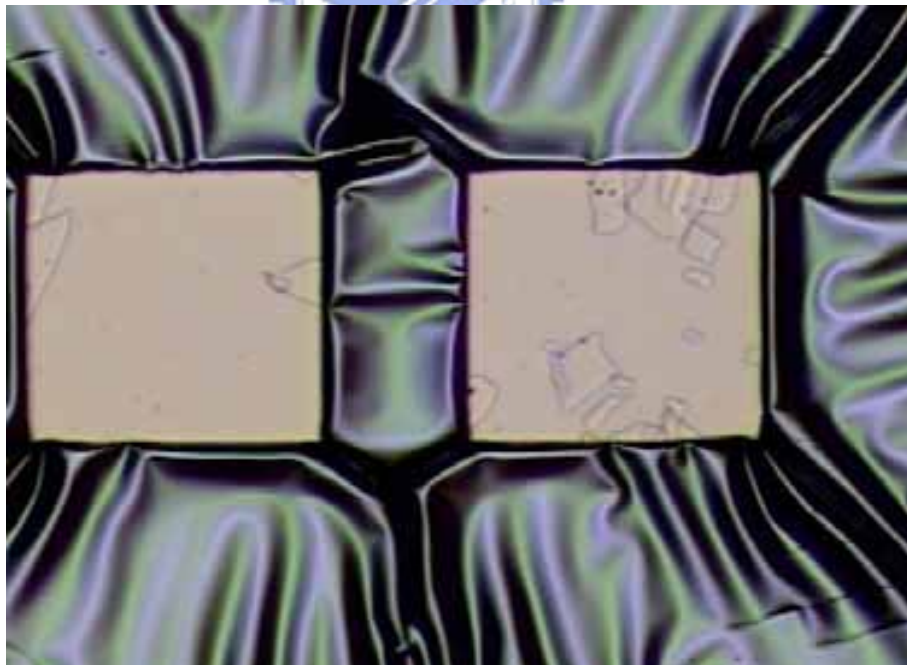
utilized as the sacrificial layer.

Figure 3-2 PR sacrificial layer after soft bake (no hard bake).

Figure 3-3 PR sacrificial layer after soft bake (hard bake less).
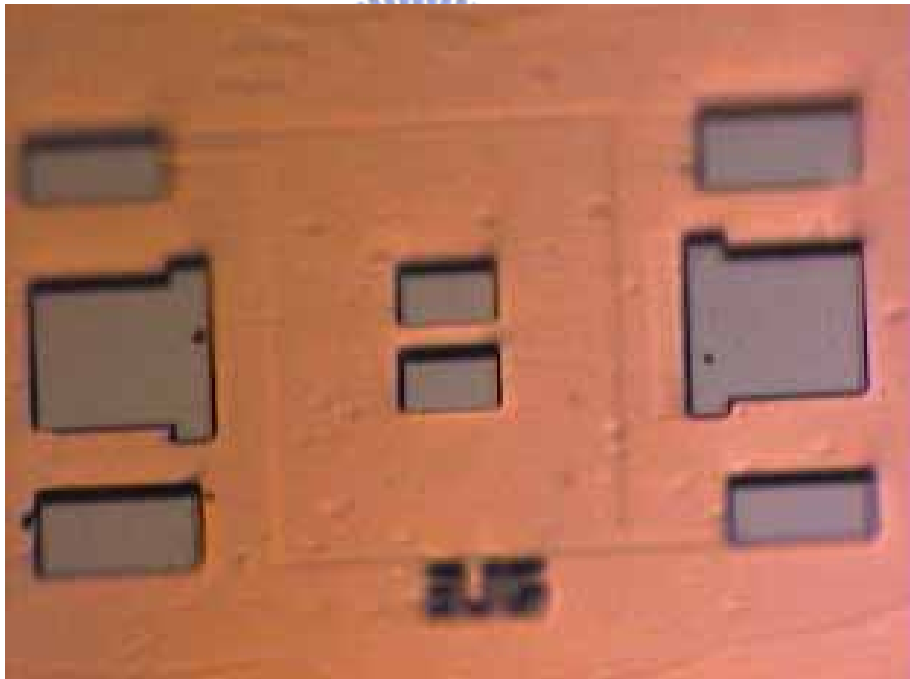

Figure 3-4 Cu sacrificial layer.

P.profile   ├────┤5mm   Diff1:22.340um   2:16.066um   3:14.452um

22mA/cm²

V.mag.20000(0.05) H.mag.1000(0.002)

P.profile   ├────┤5mm   Diff1:13.559um   2:10.778um   3:10.207um

10mA/cm²

V.mag.2000(0.25) H.mag.500(0.004)

P.profile   ├────┤5mm   Diff1:7.414um   2:6.594um   3:6.012um

5mA/cm²

V.mag.10000(0.05) H.mag.1000(0.002)
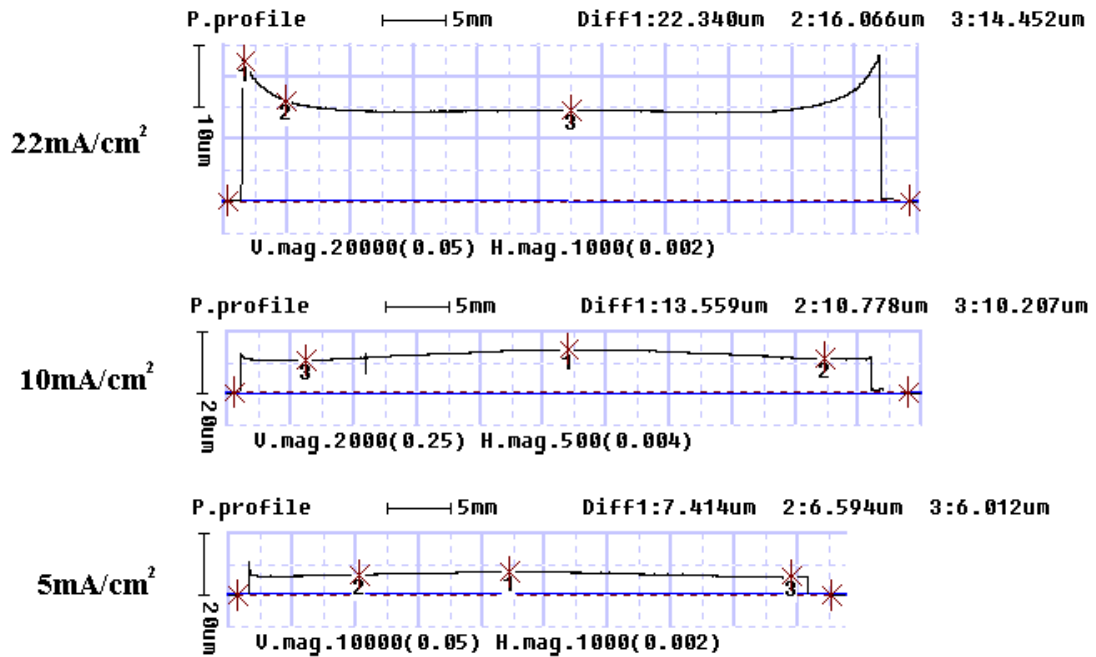
Figure 3-5 profile of Cu sacrificial layer under different current densities.

3.1.2 Process Flow

According to the mentioned above, the materials of main layers are decided. So the process flow can be determined and given below.   The relative process flow chart is shown in Figure 3-6.

Step1: After RCA cleaning, wet oxide and LPCVD nitride are deposited on the silicon substrate.   FH6400 is spun on the wafer and patterned by Mask#1.   Sputtered Ti and Ni are lifted off by FH6400. Here, Ti is the adhesion layer and Ni is the pad material.

Step2: Cu sacrificial layer-

Sputtered Ti and Cu are lifted off by FH6400 which is patterned by Mask#2. AZ4620 patterned by Mask#2 is used as the mold of the Cu electroplating.   This Cu layer is the sacrificial layer.

PR sacrificial layer-

FH6400 is spun on the wafer and patterned by Mask#2' (inverse of Mask#2). Cu is sputtered as the seed layer after hard bake.

Step3: AZ9260 is spun on the wafer and patterned by Mask#3. This AZ9260 layer is the mold of the Ni electroplating.

Step4: Ni and Ni-Diamond are electroplated by using the Cu as the seed layer.

Step5: For Cu sacrificial layer-

AZ9260 and Cu layer are removed by ACE and the solution of ammonia plus hydrogen peroxide individually. Finally, the sample is baked dry after IPA immersion.

For PR sacrificial layer-

AZ9260 and Cu seed layer are removed by ACE and the solution of ammonia plus hydrogen peroxide individually. Here the etching of the Cu seed layer must be well control. The structure may peel off because of the over etching. The FH6400 sacrificial layer is removed by PR stripper. At last, the sample is baked dry after IPA immersion.
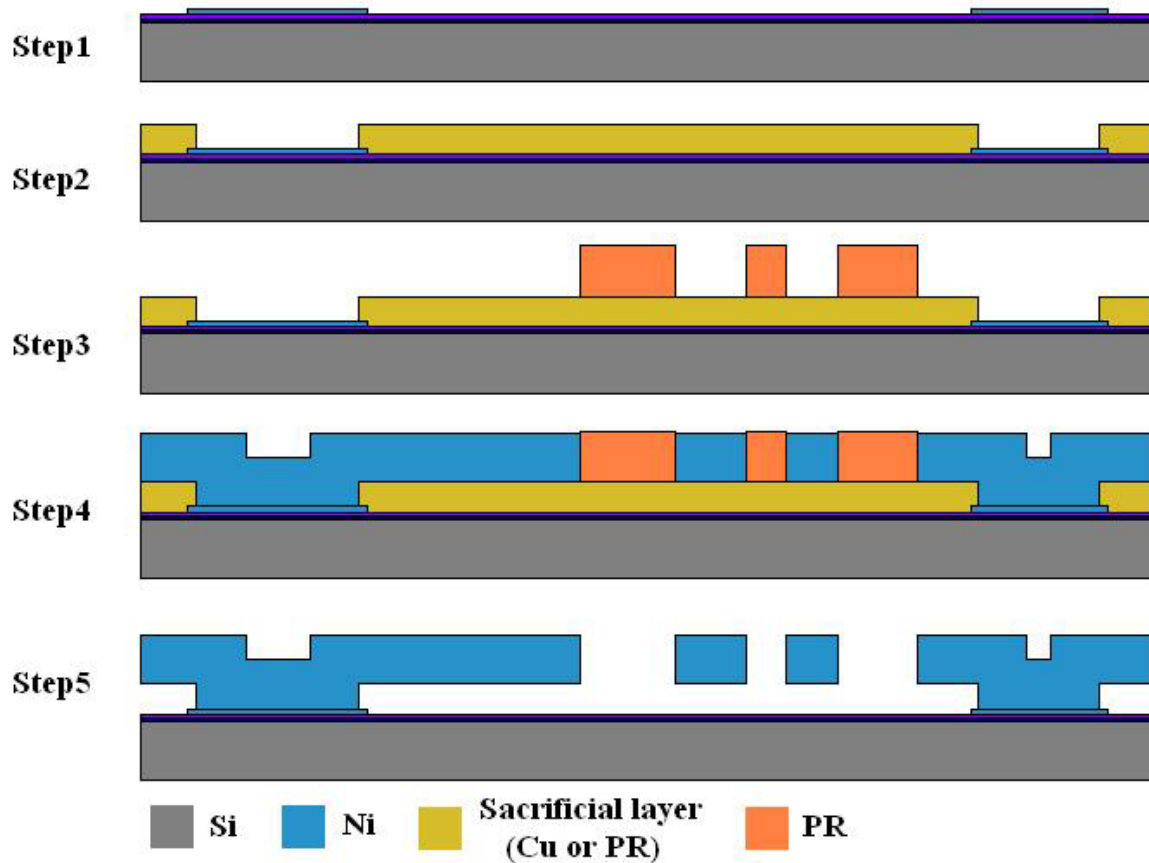
Figure 3-6 process flow chart.

3.2 Photoresist Process

Before electroplating, there must be a good PR mold.   The good PR mold is defined as the high aspect ratio, the vertical sidewall, and the less loss of linewidth.   Here the high aspect ratio can be solved by using AZ9260.

It is found that there is serious linewidth loss of the comb gap when all parts are well developed.   The result is shown in Figure 3-7.   Before the PR is spun on, there is a step height between the anchor and sacrificial layer.   After the PR is spun on, the thickness of the PR on anchor is thicker than on sacrificial layer.   In order to develop the PR in anchor well, the developed time must be extended then the linewidth of the comb gap loses.   This

problem can be solved by using plasma etching.   When the PR on sacrificial layer is well developed, the developing process stops.   The residual PR on anchor can be removed by plasma etching.   Plasma etching is anisotropic etching.   Therefore, the linewidth of comb gap won't be lost.   But there is no such equipment available.   By diluting the developer, the loss of the linewidth of comb gap can reduce.   Comparing Figure 3-8 with Figure 3-7, there is a better comb gap by diluting the developer.

AZ9260 can also solve the problem of the vertical sidewall.   As shown in Figure 3-9, the sidewall is about 80 degrees.   This result is better than what made by AZ4620.

If the mold is much thicker than electroplating film, the sidewall will more close to 90 degrees.   For example, the thickness of mold in 13μm shows better vertical sidewall than one in 7μm for the thickness of the electroplating film in 7μm.
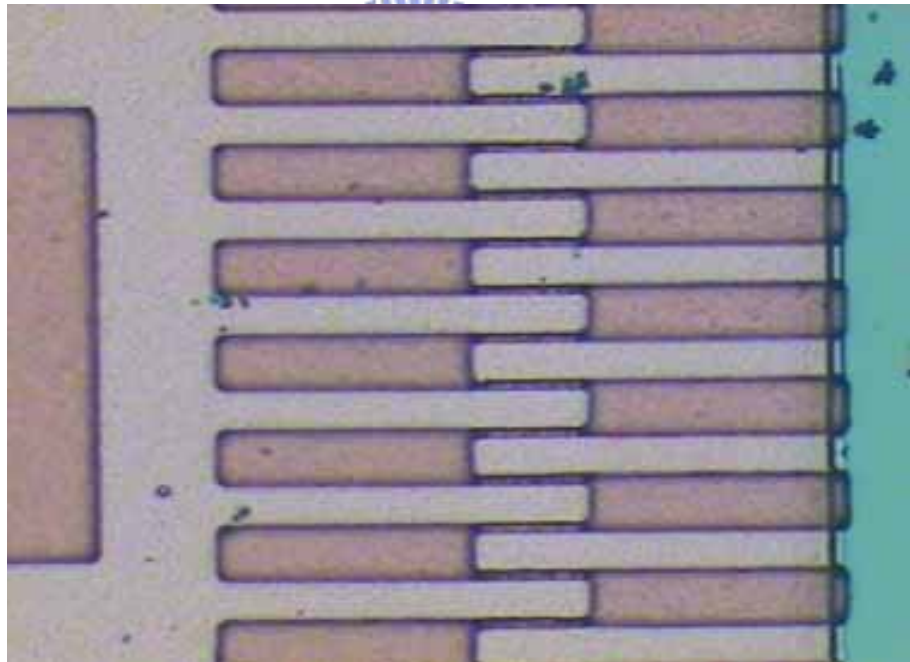

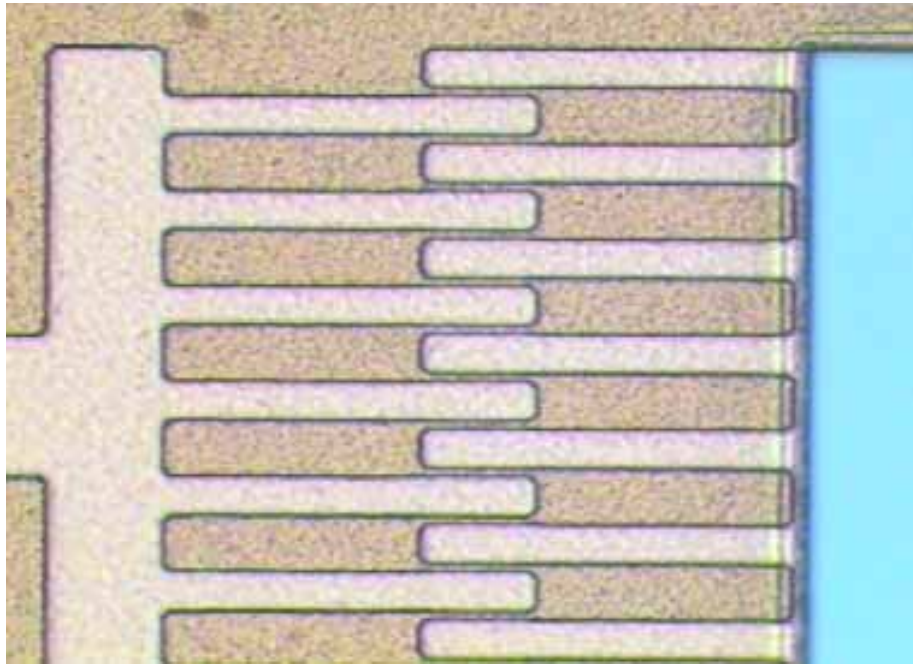Figure 3-7 AZ9260 after developed (the original comb gap is 4μm)

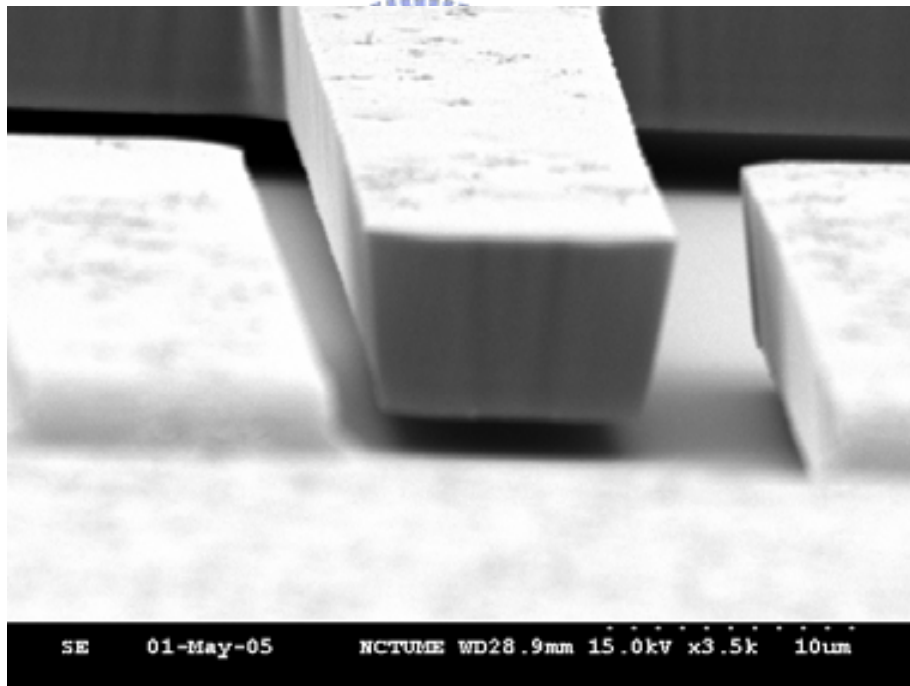Figure 3-8 AZ9260 after developed by diluting the developer (the original comb gap is 4μm)

SE   01-May-05   NCTUME WD28.9mm 15.0kV x3.5k   10um

Figure 3-9 sidewall of comb drive

3.3 Nickel and Nickel-Diamond Electroplating

Electroplating is the most important step in whole process. The quality of comb drive depends on the conditions while electroplating. Here no bending and no stiction structures are needed. By preliminary experiment result, the stiction phenomenon can be solved by IPA immersion. No bending structure depends on the residual stress of the structure and the residual stress depends on the factors of electroplating condition. There are too many factors to control the electroplating conditions. In order to finding out what the key point is, it seems useful to divide these factors into two parts. One is the electroplating solutions relative; the other is the operation condition relative.

The electroplating solution relative factors are simply defined as the quantities of the compositions and pH level. In the electroplating solution, there are nickel sulfamate, boric acid, nickel chloride, and additives. It is hard to obtain optimum situation by tuning the quantities of the compositions. So what can be done is following the commercial solutions. All the quantities of compositions are shown in Table 3-1. The pH level of the solution is kept in 4.0~4.3. The pH level of the solution which obeys Table 3-1 is at the range from 4.05 to 4.15. Sulfuric acid and ammonium hydroxide are used to counteract the solution if the pH level is over the range. The diamond nanoparticles with average diameter in 500nm are added into electroplating solution with concentration in 2g/L. The diamond nanoparticles have no influence with the pH level.

Current density, temperature, and ventilated system are the important parameters of operation condition. By changing current density and temperature, the different deposition rate and residual stress can be observed. These parameters are easier to control than those parameters of the electroplating solution relative.

Table 3-1 the quantities of compositions in the nickel electroplating solution.

composition	Nickel sulfamate	boric acid	nickel chloride	additives	
				EPC-30	NPA
quantity	400mL/L	40g/L	5g/L	10mL/L	1~3mL/L

3.3.1 Setup of the Electroplating System

The electroplating system is shown in Figure 3-10. The system includes tank, cathode part, anode part, ventilated system, pump, and power supply. The sample is pasted on the cathode part. In Figure 3-12, there is a dummy part on the cathode except the sample. The dummy part is used to increase the total area. The sample area is about 1cm^2. With 1.2mA/cm^2 current density, the operation current is 0.0012A. This current is impossible for the power supply. For this reason given above, it is necessary to increase the total area. By using the dummy area, the total area can increase to 11cm^2 and the operation current increase to 0.013A. This current is possible for the power supply.

The real nickel electroplating system is shown Figure 3-13. Because it needs heating during electroplating, the tank is immersed into the constant temperature water immersion system.
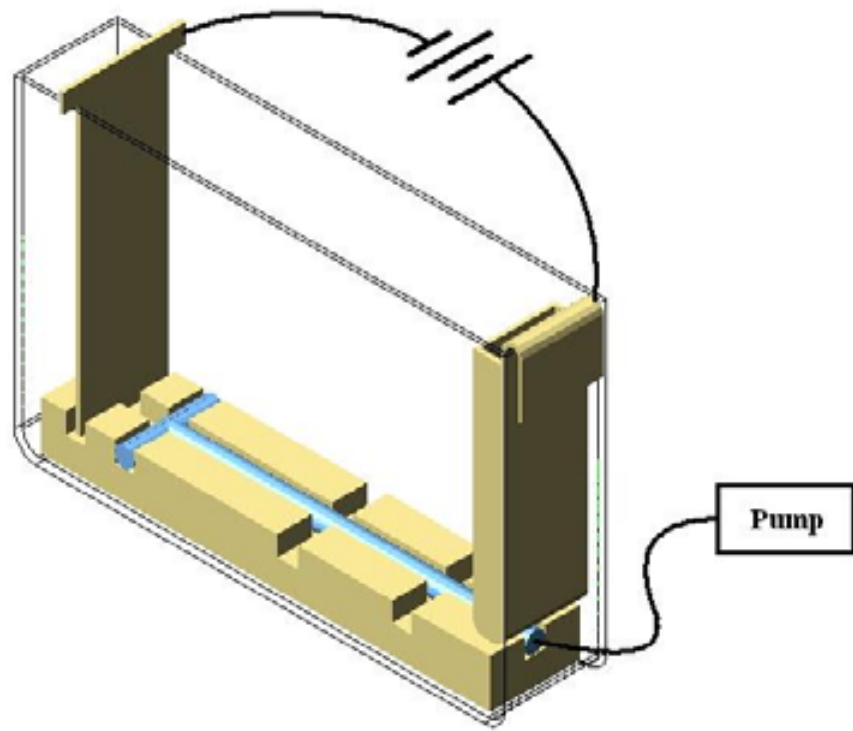
Figure 3-10 setup of the electroplating system.

(a)   (b)

<div align="center">(c)   (d)</div>

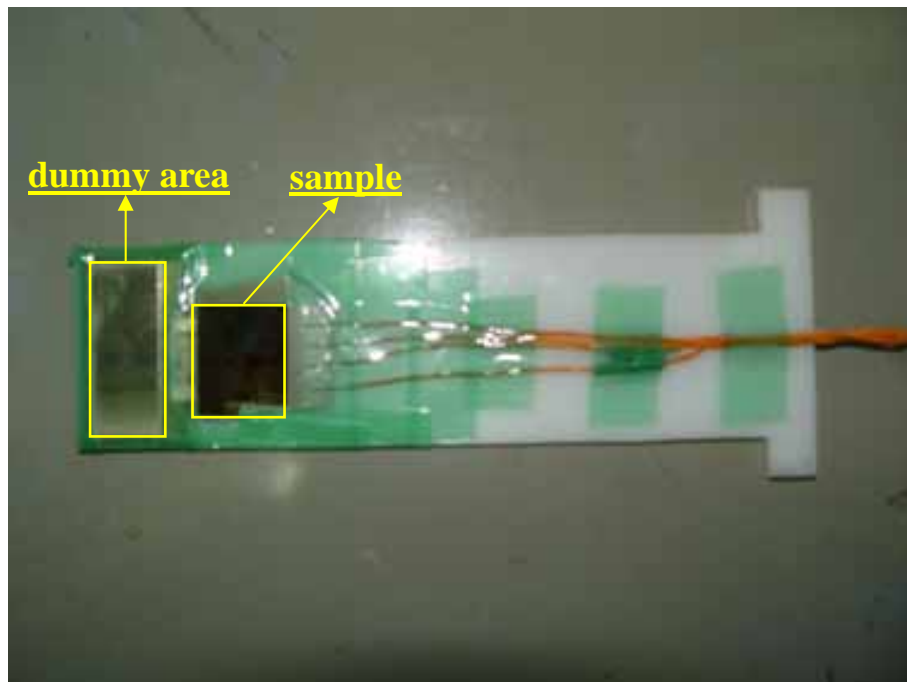Figure 3-11 (a) tank; (b) cathode part; (c) anode part; (d) ventilated system.

Figure 3-12 the cathode part with sample.

Figure 3-13 the electroplating system.

3.3.2 Current Density Effect

Current density is defined as the current dividing by the effective area. According to the experimental result, it seems helpful to reduce the residual stress by reducing the current density. According to the figure in Figure 3-14 and Figure 3-15, there is less residual stress when reducing the current density.

Except reducing the residual stress, there is one more important phenomenon when the current density is lowered down. From electroplating point of view, current density indicates how many metal atoms are precipitated per area. So the deposition rate can be easy controlled by current density. Actually, the proportion of the deposition rate to the current density isn't always the constant. Figure 3-16 shows the experimental result. The slope of low current density is sharper than high current density. The sharper slope indicates that the rate of electron transform into nickel is lowered down at low current density.

Though the bending effect can not be solved complete by reducing the current density,

the suspension structure can be obtained for pure nickel electroplating. The proper current density for nickel electroplating is 1.2mA/cm^2. This residual stress reducing effect is not effective at the current density less than 1.2mA/cm^2. For nickel-diamond, the end of the spring still touches with the substrate. In other words, the residual stress is still serious at the same condition for nickel-diamond structure. Therefore, only reducing the current density is no use for nickel-diamond structure.
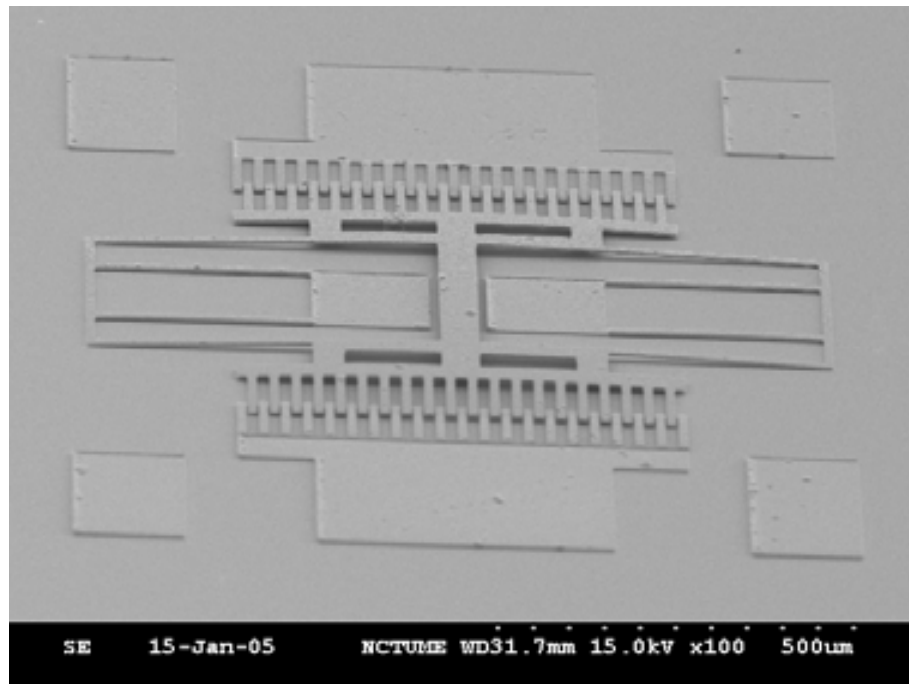

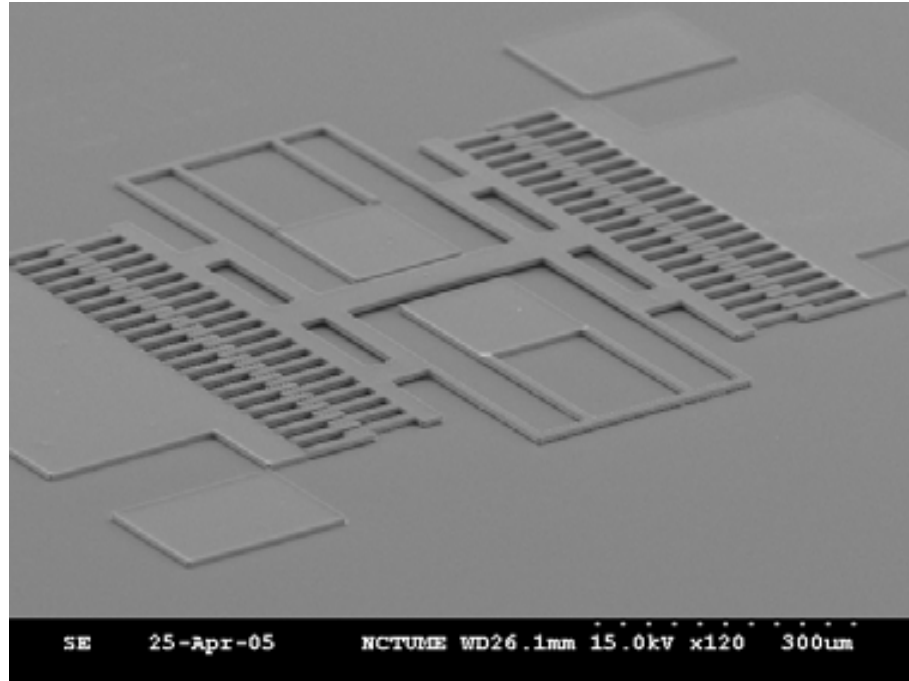Figure 3-14 nickel electroplating with high current density (22mA/cm^2).

Figure 3-15 nickel electroplating with low current density (1.2mA/cm^2).
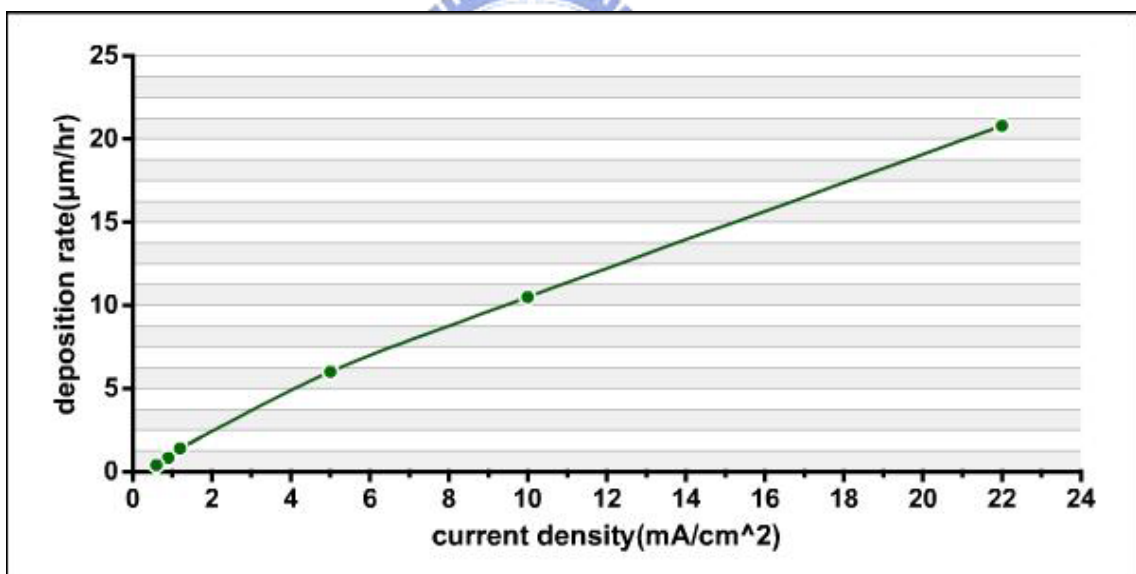

Figure 3-16 current density-deposition rate for nickel electroplating.

3.3.3 Temperature Effect

By changing the operation temperature, it is found that the suspension nickel-diamond can be obtained. There are two reasons. One is that temperature causes geometry

28

deformation and the other is that temperature causes the variation of residual stress.

Based on the equation of the thermal expansion, the elongation of the beam grows with the increases of the temperature difference, the original length of the beam, and the thermal expansion coefficient. It is shown in the following equation:

$$\Delta L = L_0 \alpha \Delta T \qquad (3.1)$$

Where ΔL, L_0, α, and ΔT represent elongation, original length, thermal expansion coefficient, and temperature difference. In the standard nickel electroplating process, the operation temperature must be retained at 50 . If the room temperature is 25 , there is 25 temperature difference. So there must be elongation under nickel electroplating process.

The spring beams of comb drive can be considered as long-short. According to the equation, the expansion deviation of long beam and short beam can be represented as $L_c \alpha \Delta T$. L_c is represented as the difference between the long beam and short beam. The expansion deviation may cause the bending of spring beams. The dimension and the material are decided, so the expansion deviation is reduced only by decreasing the operation temperature.

But by heating the released sample to 80 , the bending effect is not serious. The result is shown in Figure 3-17. Except the geometry deformation, the changing of temperature also causes different residual stress.
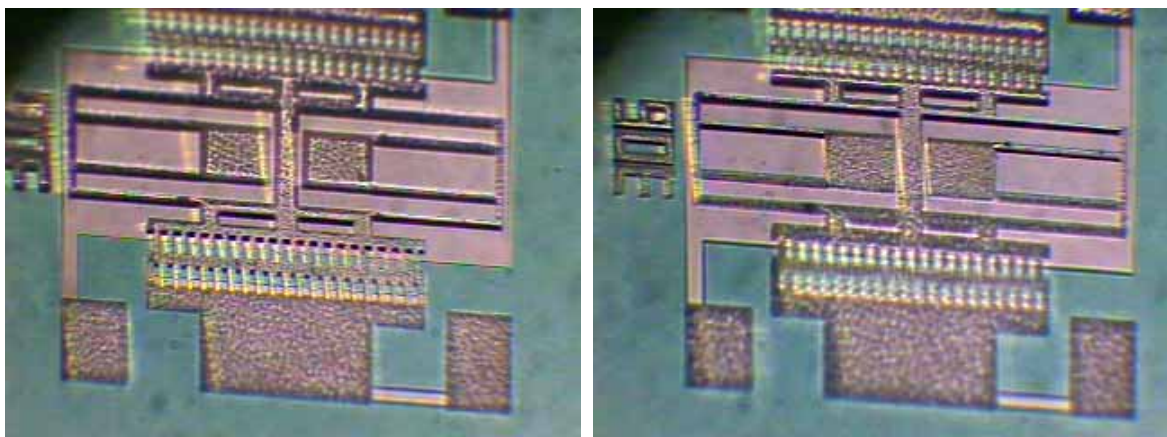

(a)   (b)

Figure 3-17 comb drive (a) at room temperature; (b) at 80 .

29

3.4 Results of Electroplating

As mentioned above, it is useful to achieve the suspension structure by reducing the current to 1.2mA/cm^2 and lowering the operation temperature to 35 . The structures are shown in Figure 3-18 and Figure 3-19. By pure nickel electroplating, there is a smooth surface. Next turning nickel-diamond electroplating, the surface of comb drive is dispersed by voids.

Except pure nickel and nickel-diamond, there is a test for nickel-CNT electroplating. It is found that the structure is still bending under the same fabrication process. The result of nickel-CNT electroplating is shown in Figure 3-20.
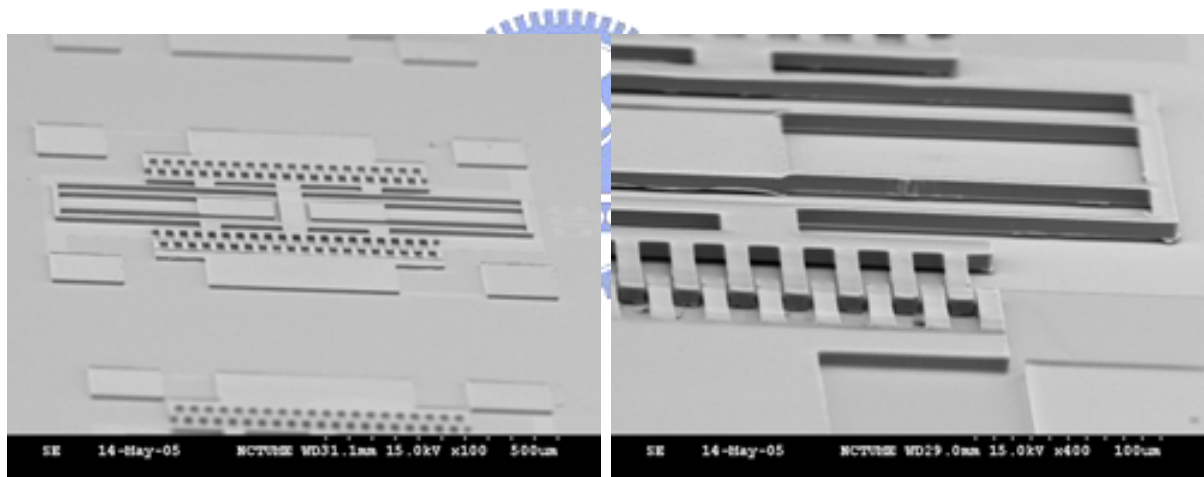
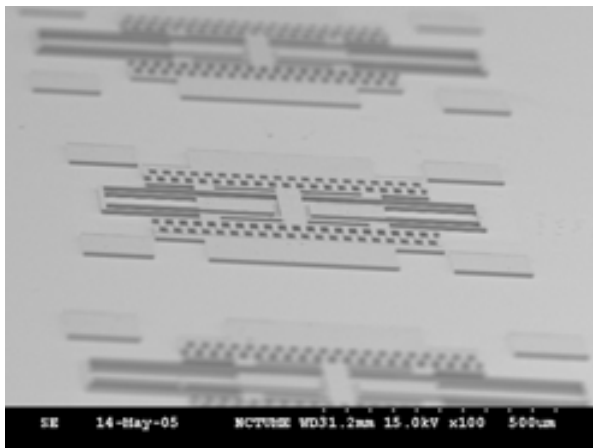(a)   (b)
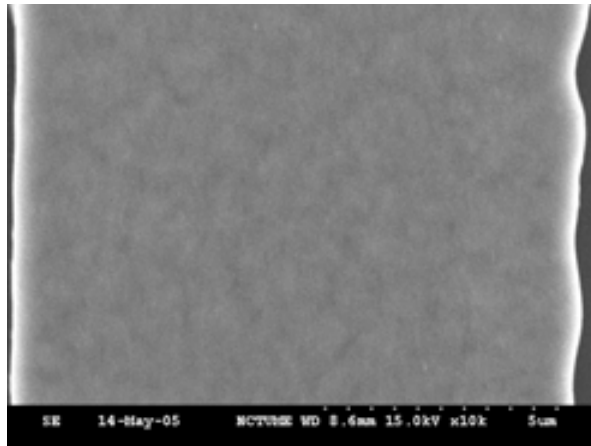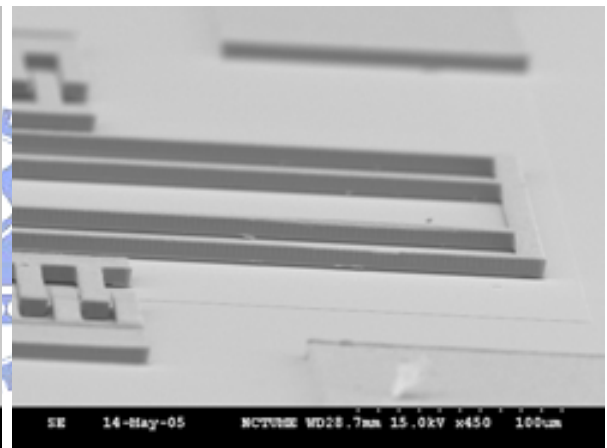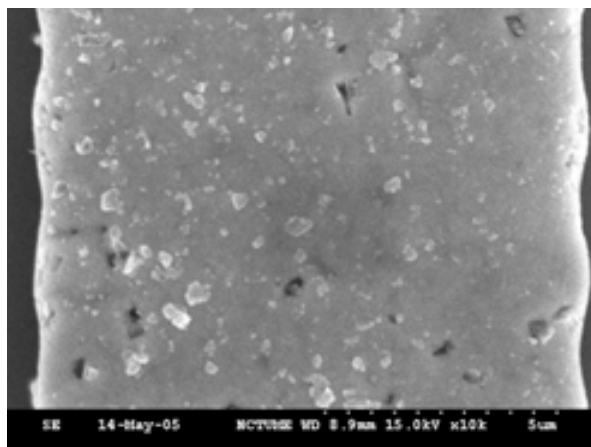
(c)

Figure 3-18 (a) full view; (b) spring part; (c) surface of comb drive by pure nickel
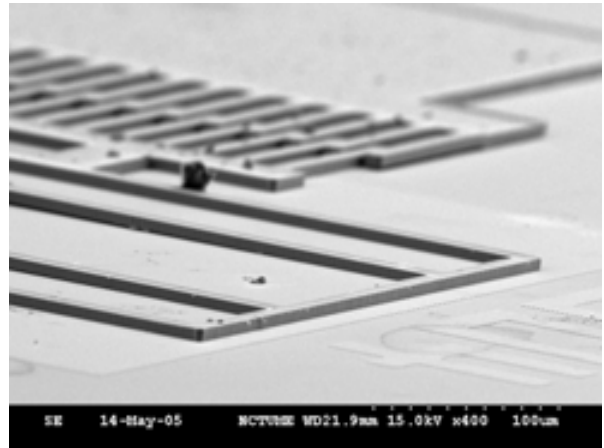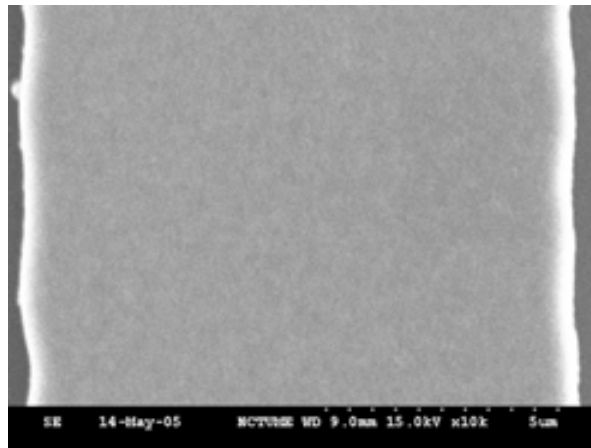

(a)

(b)

(c)

Figure 3-19 (a) full view; (b) spring part; (c) surface of comb drive by nickel-diamond

(a)

(b)

(c)

Figure 3-20(a) full view; (b) spring part; (c) surface of comb drive by nickel-CNT

Chapter 4 Measurement and Discussion

4.1 Material Property Measurement

The suspension comb drive structure is fabricated by the process flow mentioned above. Although the electroplating solution is the same, the material by these operation conditions is different from Teh's research. In Figure 4-1, it shows the diamond nano particles are not easy to be fu in Teh's research. This phenomenon is different from the random distribution in Figure 3-19(c). In Shen's research, the diamond nano particles induce the creaks and voids in the nickel film. There are only voids in Figure 3-19(c). The material properties may be different from Teh's and Shen's. So it is necessary to measure the material property.

(a)   (b)
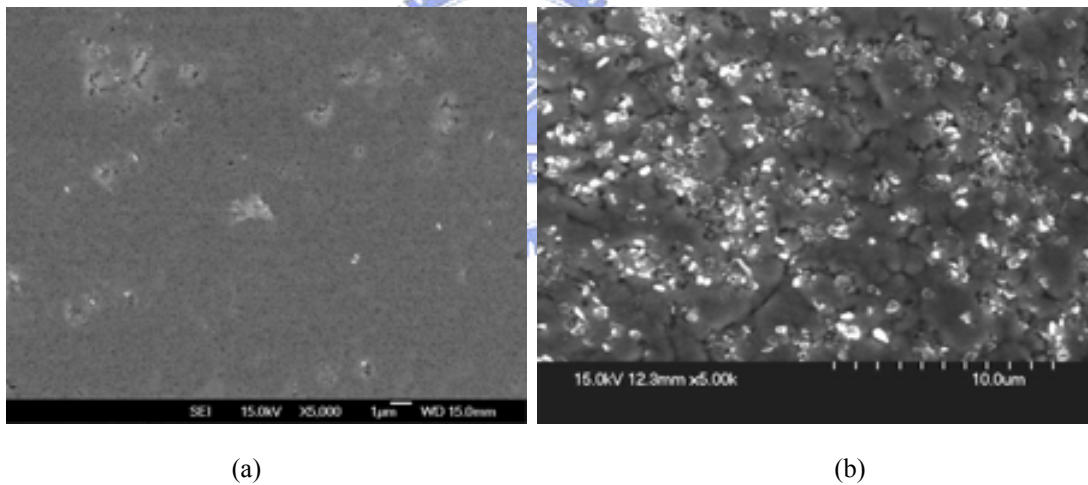
Figure 4-1 (a) TEM photo of nickel-diamond in Teh's research[13]; (b) SEM photo of

nicke-phosphorus-diamond in Shen's research[14].

4.1.1 Measurement of CTE

By heating the sample, there is length difference between room temperature and higher temperature. Here the highest temperature is 350℃ and the heating process is recorded by

CCD.

According to the recorded film, each length of beam can be expressed as pixels.　Using these pixels difference and substituting into equation (3.1), the CTE is shown in Table 4-1. This CTE measurement is at 350℃　because the pixel difference is hard to distingue at lower temperature.

The result shows that the nickel-diamond nanocomposite has higher CTE than pure nickel.　This tendency is the same as the Teh's researches.

Table 4-1 the results of CTE measurement.

|	number	1	2	3	4	5
pure nickel	L0(pixels)	363	363	359	362	362
	L1(pixels)	364	364	360	363	364
	ΔL(pixels)	1	1	1	1	2
	ΔT( )	320	320	320	320	320
	α(10-6/)	8.6	8.6	8.7	8.6	17.2
	average α(10-6/)	10.4				
nickel-diamond	number	1	2	3	4	5
	L0(pixels)	362	362	360	362	362
	L1(pixels)	366	365	365	366	365
	ΔL(pixels)	4	3	5	4	3
	ΔT( )	320	320	320	320	320
	α(10-6/)	34.5	25.9	43.4	34.5	25.9
	average α(10-6/)	32.9				

4.1.2 Measurement of Young's Modulus and Hardness

Young's modulus is an important property and this property can be measured by nano indenter. By indenting the sample form surface to the setting depth, the relation of Young's modulus and depth can be obtained. The results of pure nickel and nickel-diamond are shown in Figure 4-2 and Figure 4-3. One line represents the result of one location of the sample. According to the experiences, different location and depth get different Young's modulus. So it is necessary to take more locations to get more reliable average results. There are sixteen locations taken and the depth is set at 700nm. The results show the Young's modulus from surface to 700nm. By renouncing the curve with strange shape, the finial results are taken from 500nm to 700nm because it may be some problems at initial measurement. The curve with strange shape may be caused from slide of the needle. Except Young's modulus, the hardness can also be obtained by nano indenter. The results are arranged in Table 4-2.
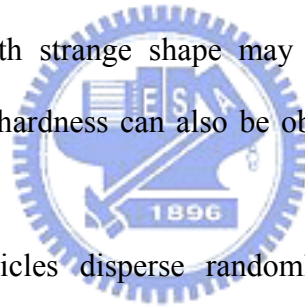
The diamond nano particles disperse randomly in nickel film and the diamond concentration of one location has some different from each other. Therefore, the property measurement of nickel-diamond gets larger deviation than pure nickel.
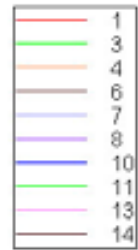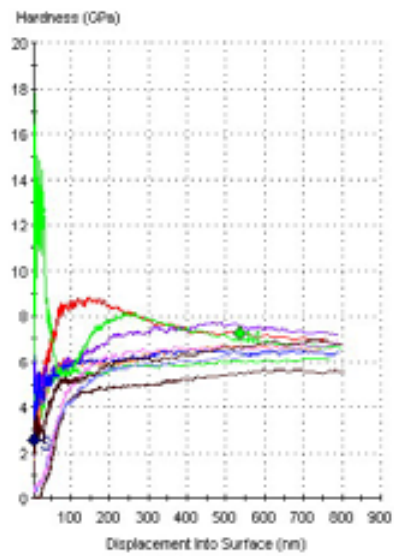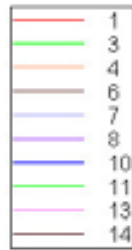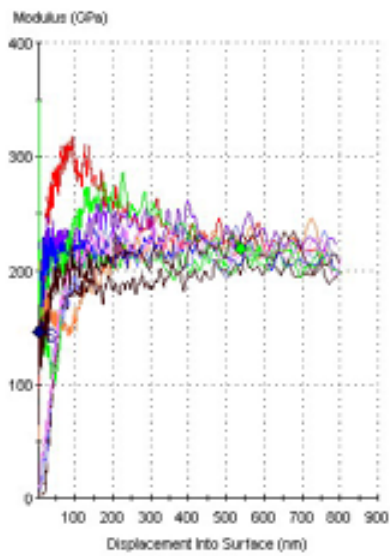
The results show that the Young's modulus of nickel with diamond nano particles in it is improved from 173GPa to 217GPa.
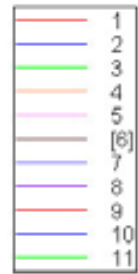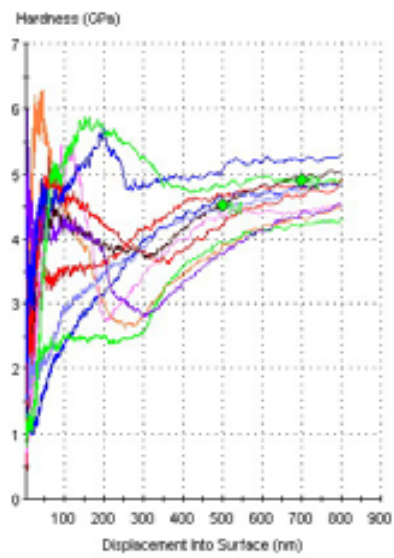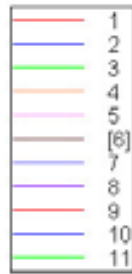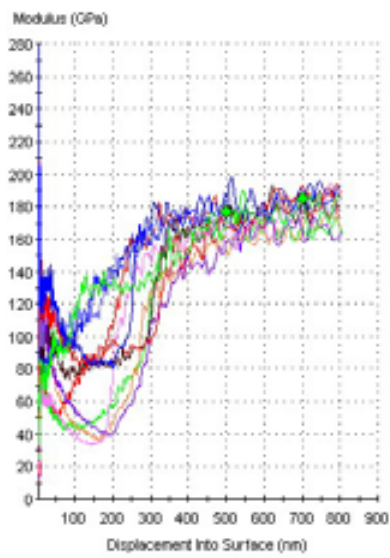
(a)   (b)

Figure 4-2 (a) Young's modulus and (b) hardness of pure nickel.

(a)   (b)

Figure 4-3 (a) Young's modulus and (b) hardness of nickel-diamond.

Table 4-2 the results arrangement of Young's modulus and hardness.

material	property			
	Young's modulus (GPa)		Hardness (GPa)	
pure nickel	average	standard deviation	average	standard deviation
	173	6.57	4.5	0.35
nickel diamond	average	standard deviation	average	standard deviation
	217	8.82	6.6	0.54

4.2 Resonant frequency measurement

The Laser Doppler Vibrometer (LDV) is used to measure the resonance.   This instrument can observe the displacement under different frequency.   When comb drive is operated under resonant frequency, it is easy to found large displacement.   According to this concept, the resonant frequency can be found by the obvious displacement shift.

There are two main measurements of motion: in-plane and out-of-plane.   LDV is an ideal tool for displaying out-of-plane displacement.   It is impractical to measure in-plane motion since the Doppler shift is derived from a velocity vector normal to the plane of the moving surface.   The problem of in-plane motion measurement can be solved by using stroboscopic video microscopy.   The resolutions of in-plane and out-of-plane are 20nm and 0.5nm.

By preliminary test, the in-plane displacement of comb drive in this thesis is too small to observe.   Although the comb drive is designed to move only in the in-plane direction, some residual out-of-plane motion exists that can be detected through the high sensitivity of the LDV sensor.   Therefore the out-of-plane measurement is used to find the resonant frequency and the operation condition is set under 50V AC with 50V DC bias.

The displacements of comb drive made by pure nickel are shown in Figure 4-4. The frequency range is from 1kHz to 21kHz for the spring with 300μm in length. It seems that there is a main peak at 7~8kHz. This peak is the first mode. After this peak, there are two peaks combining from 17kHz to 20kHz. These two peaks may be the second and third modes. The peaks of second and third modes are not easy to recognize. So the measurement is focused on the first peak.

In order to find the more accurate position of resonant frequency, it is necessary to take more points on the possible location. Figure 4-5 is based on Figure 4-4 to take 30 points from 7kHz to 10kHz. It seems that the first mode of pure nickel comb drive is located at 8.034kHz. The same steps are applied on nickel diamond comb drive. Referring to Figure 4-6 and Figure 4-7, it is found that the first peak is located at 8.949kHz. The peak of nickel diamond comb drive is not obvious. By the measurement results, it seems that the nickel diamond comb drive gets smaller displacement than the pure nickel one. Because the spring constant of nickel diamond one is larger the pure nickel one, the nickel diamond one gets small displacement under the same operation condition.

As shown in Table 4-3, the results measured by LVD are larger than the simulation results. This phenomenon can be explained by the spring size. The sidewall of simulation modal is vertical but the actual sidewall is about 80 degrees. It make the spring constant of actual comb drive larger than ideal one. So it is reasonable to get large resonant frequency by measurement.
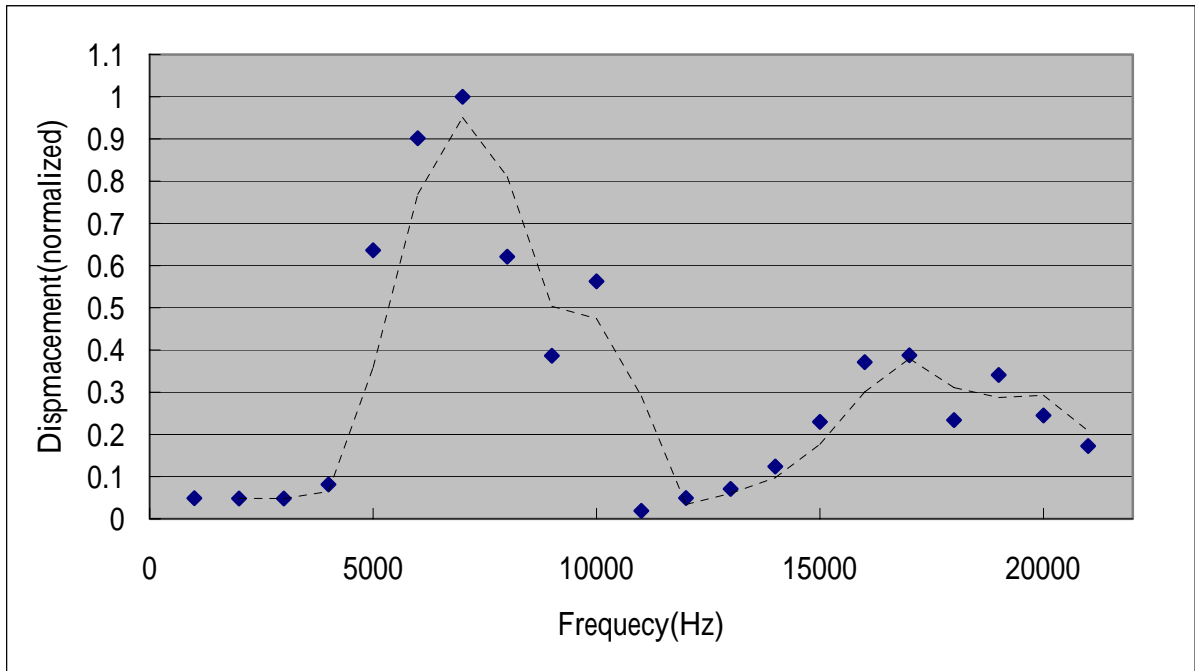
Figure 4-4 Frequency-Displacement relation of pure nickel comb drive form 1kHz to 21kHz.
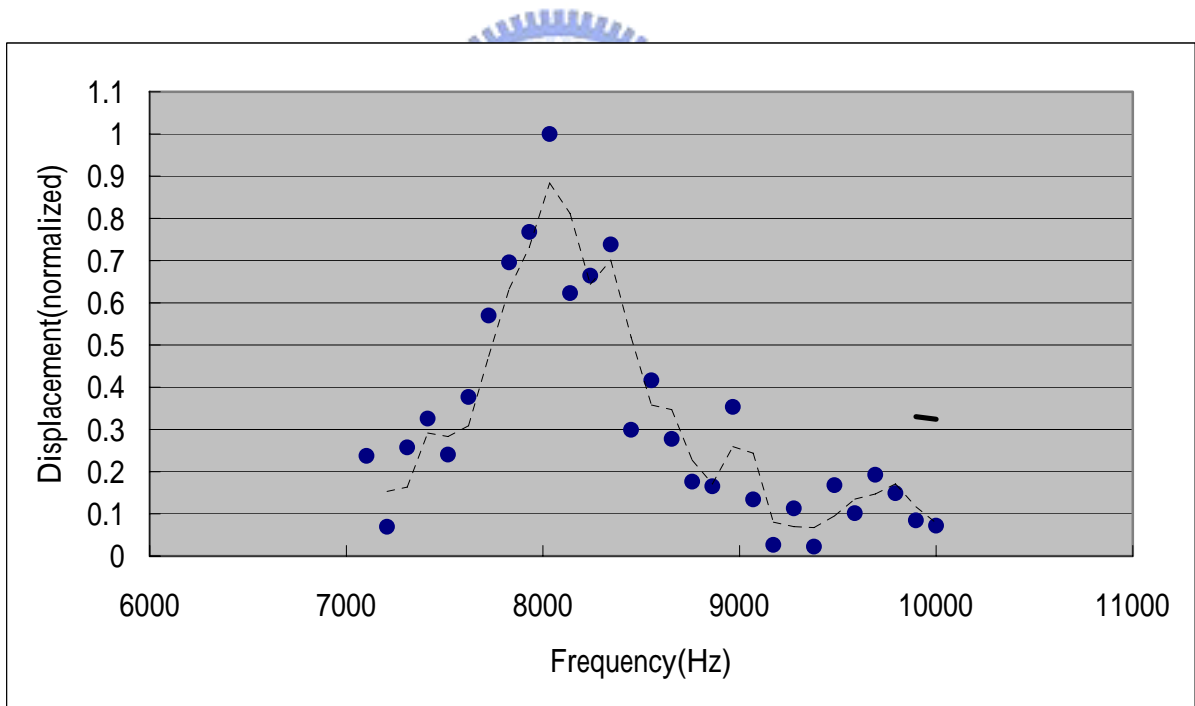
Figure 4-5 Frequency-Displacement relation of pure nickel comb drive form 7kHz to 10kHz.
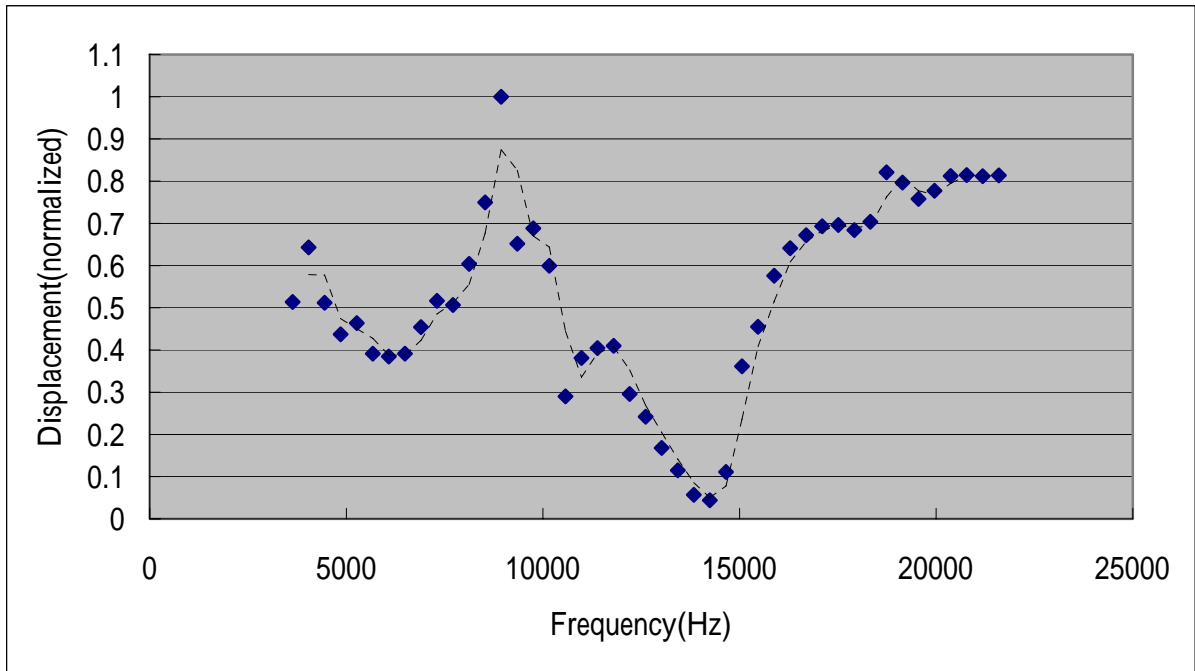
Figure 4-6 Frequency-Displacement relation of nickel diamond comb drive form 3kHz to 22kHz.

Figure 4-7 Frequency-Displacement relation of nickel diamond comb drive form 7kHz to 10kHz.

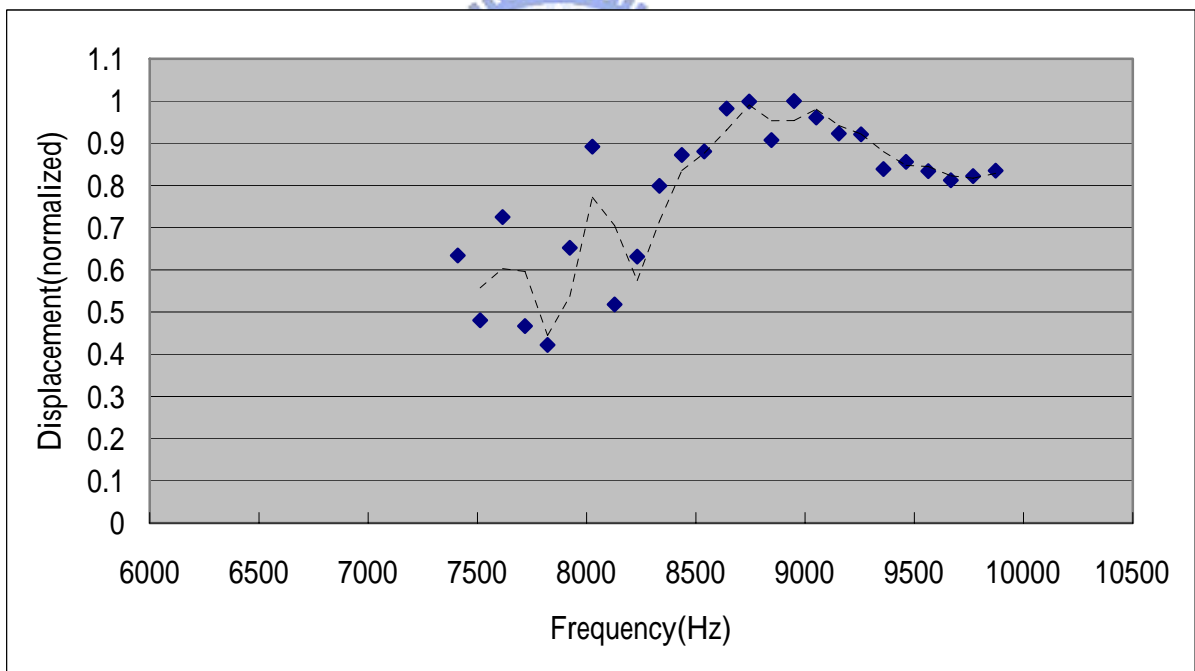Table 4-3 resonant frequency deviation between simulation and measurement.

material	first mode	
	simulation (Hz)	measurement (Hz)
pure nickel	6804	8034
nickel diamond	7497	8949
Improvement (%)	10.2	11.4

Chapter 5 Conclusion

The comb drives made by pure nickel and nickel diamond are demonstrated by electroplating.　There are some important points in fabrication and measurement.

By reducing the current density and operation temperature, it is possible to eliminate bending in comb drive structure.　Except the two parameters, there are many other conditions which can be tuning.　For example, the composition and pH level of the electroplating solution are the tuneable parameters.　Under $1.2mA/cm^2$ and 35 , it is possible to get the structure with no bending.

The material properties are a little bit difference between different operation parameters. This is a serious problem for electroplating.　In order to get comparable device, the comb drive made by pure nickel or nickel diamond is under the same operation conditions.

In the measurement side, there are many driving methods in the relative literatures.　It seems that only one of these methods can drive the comb drive in this thesis.　So it is needed to confirm the drive methods.

The dimension design is an important issue of comb drive manufacture.　The dimensions of comb drive in this thesis are based on the fabrication ability, so it is hard to reduce the dimensions.　According to the experiment experience, some related problems may be solved by reducing the dimensions.　For example, if the width of spring is reduced, the thickness can also be cut down and the operation time can be diminished.　If the thickness is much larger than the width of spring, the in-plane mode would occur before the out-of-plane mode and there is no coupling of the in-plane and out-of-plane mode.　The linewidth also influence the electrostatic force.　It is found that the electrostatic force of comb drive in this thesis is too small to drive comb drive because the gap of comb structure is too large.　By reducing the gap of comb structure, the electrostatic force can be improved

effectively.   So it is necessary to find another aligner which can get smaller linewidth for further research.

Reference

[1] W. C. Tang, T.-C. H. Nguyen, and R. T. Howe, "Laterally Driven Polysilicon Resonant Microstructure", Proceedings IEEE MEMS, February, 1989, pp.53-59.

[2] M. Biebl, G. T. Mulhern, and R. T. Howe, "In Situ Phosphorus-Doped Polysilicon for Integrated MEMS", the 8th International Conference on Solid-State Sensors and Actuators, and Eurosensors IX. Stockholm, Sweden, June 25-29, 1995, pp. 198-201.

[3] Franke, A.E.; Bilic, D.; Chang, D.T.; Jones, P.T.; King, T.-J.; Howe, R.T.; Johnson, G.C. "Post-CMOS Integration of Germanium Microstructures" 12th IEEE Int. Conf. on Micro Electro Mechanical Systems (MEMS 99), Orlando, Florida, Jan. 17-21, 1999, pp. 630-637.

[4] S.-A. Bhave, B.-L. Bircumshaw, W.-Z. Low, Y.-S. Kim, Albert P. Pisano, T.-J. King, and R. T. Howe, "Poly-SiGe: A High-Q Structural material for Integrated RF MEMS", Solid-State Sensor, Actuator and Microsystem Workshop Hilton Head Island, South Carolina, June 2-6, 2002, pp. 34-37.

[5] D. Gao, M.B.J. Wijesundara, C. Carraro, C.W. Low, R.T. Howe, and R. Maboudian, "High Modulus Polycrystalline 3C-SiC Technology for RF MEMS", Proc. Transducers'03, The 12th International Conf. Solid-State Sensors & Actuators, pp. 1160-1163.

[6] B. Kim ; S. Park, H. Kim, K. Chun, D.-I. Cho, J.-W. Lee, H.-J. Lee ; W.-K, Seong, Y.-J. An, "MEMS Fabrication of High Aspect Ratio Track-Following Micro Actuator for Hard Disk Drive Using Silicon on Insulator" IEEE International Conference on Micro Electro Mechanical Systems, Jan. 1999, pp.53-56.

[7] K.-H. Jeong and Luke P. Lee, "A Novel Fabrication Method of a Vertical Comb Drive Using a Single SOI Wafer for Optical MEMS Application", in Proc. 2003 Int. Conf. Solid-State Sensors and Actuators, pp. 1462-1465

[8] A. D. Yalcinkaya, S. Jensen, and O. Hansen, "Low Voltage, High-Q SOI MEMS Varactors

for RF Application", Proceedings of the 29th EuropeanSolid-State Circuits Conference, ESSCIRC 2003,Estoril, Portugal, September 16 - 18, 2003, pp. 607-610

[9]W.-T. Hsu and Clark T.-C. Nguyen, "Geometric Stress Compensation for Enhanced Thermal Stability in Micromechanical Resonators", Proc. of 1998 IEEE Int. Ultrasonics Symposium, Sendai, 1998, pp. 945-948.

[10]A.D. Yalcinkaya, J.T. Ravnkilde, L.S. Johansen, O. Hansen, "Methods for Fabrication of Released Nickel Comb-Drive Devices on CMOS", Transducers '01, Digest of Technical Papers, Springer-Verlag, Munich 2001, pp. 600-603.

[11]K.-S. Teh, Y.-T. Cheng, and C. Sambucetti, "Selective Plating of Nickel Ceramic Composite Films for MEMS Application", Proc. 15th Annual Int. Conference on Micro Electro Mechanical System, pp.384-387, Las Vegas, NV. USA, 2002, pp. 384-387.

[12]K.-S. Teh, Y.-T. Cheng, and L.-W. Lin, "Nickel Nano-Composite Film for MEMS Application", the 12th International Conference on Solid State Sensors, Actuators and Microsystem, Boston, June 8-12, 2003, pp. 1534-1537.

[13]L.-N Tsai, G.-R. Shen, Y.-T. Cheng, W.-S. Hsu, "Power and Reliability Improvement of an Electro-Thermal Microactuator Using Ni-Diamond Nanocomposite", the 54th Electronic Components and Technology Conference, June 1-4, 2004, Caesars Palace, Las Vegas, Nevada USA.

[14]G.-R. Shen, "Properties Enhancements of Ni-P-CNTs and Ni-P-Diamond Nanocomposites Films and the applications on MEMS device", Thesis of Department of Electronics Engineering & Institute of Electronics, National Chiao-Tung University, June 2004.